

RESEARCH

Open Access



# Spatial patterns and ecological drivers of tropical moist forest transitions in the Kahuzi Biega National Park landscape eastern Democratic Republic of Congo

Nadège Cizungu Cirezi<sup>1,2,3\*</sup>, Yannick Mugumaarhahama<sup>3</sup>, Yannick Sikuzani Useni<sup>4</sup>, Cléoplace Citwara Bayumbasire<sup>1,2</sup>, Katcho Karume<sup>3</sup>, Raymond Sinsi Lumbuenamo<sup>2</sup>, Jean-François Bastin<sup>1</sup> and Jan Bogaert<sup>1</sup>

\*Correspondence:

Nadège Cizungu Cirezi  
nadegecirezi@gmail.com

<sup>1</sup>Biodiversity, Ecosystems and Landscape Unit, TERRA Teaching and Research Center, Gembloux Agro-Bio Tech, University of Liège, 5030 Gembloux, Belgium

<sup>2</sup>Ecole Régionale Post-Universitaire d'Aménagement et de Gestion Intégrés des Forêts et Territoires Tropicaux (ERAIFT), P.O. Box 15373, Kinshasa, Democratic Republic of Congo

<sup>3</sup>Department of Natural Resource Management, Faculty of Agricultural and Environmental Sciences, Université Evangélique en Afrique, P.O. Box 3323, Bukavu, Democratic Republic of Congo

<sup>4</sup>Ecology, Ecological Restoration and Landscape Unit, Faculty of Agronomic Sciences, Université de Lubumbashi, P.O. Box 1825, Lubumbashi, Democratic Republic of Congo

## Abstract

Kahuzi-Biega National Park (KBNP) is recognised as a Key Biodiversity Area for its large tracts of undisturbed tropical moist forest (UTMF) and exceptional wildlife. Since 1996, civil unrest and armed incursions have placed severe pressure on these forests, accelerating both degradation and outright loss. In this study, we examined how UTMF has changed across the KBNP landscape between 1990 and 2023, with the goal of identifying the main transition pathways and their underlying drivers. We used 30-m resolution Landsat land-cover maps from Vancutsem et al. (2021) together with field observations covering 15.7 ha to construct a 33-year transition matrix. Ten most common pathways were analysed in detail. For each, 600 pixels of interest were sampled and surrounded by three spatial windows (90×90 m, 270×270 m, 810×810 m) to calculate patch density, largest patch index, and total edge length. We also measured altitude and distances to roads, settlements, mines, and burned areas, and tested their influence using logistic regression. Results show that degradation accounted for 10.2% of transitions and direct deforestation for 5.8%. Stable UTMF occurred in homogeneous landscapes with high largest patch index and low edge length. Degradation was concentrated at low altitudes close to roads, while deforestation was more frequent at higher altitudes near burn scars. Zones of secondary-forest regrowth tended to lie in remote, inaccessible terrain. The mapped hotspots highlight priority areas where reinforcing conservation measures could help protect the park's remaining intact forest.

**Keywords** Tropical moist forest (TMF), Land-cover transition matrix, Pathway dynamics, Logistic regression, Landscape metrics, Kahuzi-Biega National Park

## 1 Introduction

Tropical moist forests are among the most ecologically significant ecosystems on Earth, playing a central role in regulating climate, storing carbon, cycling water and nutrients, and maintaining global biodiversity [36, 75]. They harbour more than half of all known



© The Author(s) 2025. **Open Access** This article is licensed under a Creative Commons Attribution-NonCommercial-NoDerivatives 4.0 International License, which permits any non-commercial use, sharing, distribution and reproduction in any medium or format, as long as you give appropriate credit to the original author(s) and the source, provide a link to the Creative Commons licence, and indicate if you modified the licensed material. You do not have permission under this licence to share adapted material derived from this article or parts of it. The images or other third party material in this article are included in the article's Creative Commons licence, unless indicated otherwise in a credit line to the material. If material is not included in the article's Creative Commons licence and your intended use is not permitted by statutory regulation or exceeds the permitted use, you will need to obtain permission directly from the copyright holder. To view a copy of this licence, visit <http://creativecommons.org/licenses/by-nc-nd/4.0/>.

terrestrial species [29, 32, 33, 38, 60] and deliver a wide array of ecosystem services, including food provision, medicinal resources, cultural values, and climate-change mitigation [43, 61, 100]. These forests also act as buffers against extreme weather events, maintain hydrological stability, and sustain millions of rural livelihoods.

The Democratic Republic of Congo (DRC) contains approximately 10% of the planet's tropical moist forests [90], forming the second-largest tropical forest block after the Amazon [1, 49, 65] and encompassing over half of the Congo Basin's most intact and ecologically valuable forests [40, 97]. The DRC is therefore pivotal in conserving contiguous tropical forest and supplying critical ecosystem services [45, 66, 89, 101]. Yet, these forests are increasingly threatened by agricultural expansion, timber extraction, mining, infrastructure development, and more frequent fires, pressures amplified by poverty, rapid population growth, and political instability [74, 87, 96, 100, 101]. Annual forest losses have averaged close to one million hectares since 2014 [52].

To counter these pressures, the DRC has established an extensive protected area (PA) network covering ~13.5% of the national territory [112]. PAs are central to tropical biodiversity conservation [15, 38] and have been shown to reduce forest loss and degradation [18, 25, 81, 116] and contribute to climate-change mitigation [12]. These areas are classified according to IUCN categories I–VI [28]. Among them, the Kahuzi-Biega National Park (KBNP), a Category II protected area and UNESCO World Heritage Site since 1996 [23], covers 6700 km<sup>2</sup> and contains diverse habitats from lowland rainforest to Afro-montane woodlands [94]. It is recognised as a Key Biodiversity Area [102] and ranks second in the Albertine Rift for endemic and threatened species, notably the critically endangered eastern lowland gorilla (*Gorilla beringei graueri*) [79, 103, 104].

Despite this status, the KBNP undisturbed forest block, identified as the park's second conservation [48], is under severe anthropogenic pressure. Since the mid-1990s, armed conflicts, population displacement, and increased accessibility have driven illegal settlement, agricultural expansion, bushfires, timber harvesting, artisanal mining, and late invasion by the liana *Sericostachys scandens* as an ecological response to disturbances [20, 51, 78]. These threats, compounded by poaching, led to KBNP's inclusion on the UNESCO List of World Heritage in Danger in 1997 [48, 93, 103]. Between 1990 and 2023, the park lost ~10% of its high-integrity tropical moist forest within its boundaries and 23% across the wider landscape [107].

At broader scales, numerous studies have investigated the drivers of tropical forest loss and degradation, both globally [2, 4, 14, 45, 57, 100, 107] and regionally [47, 53, 55, 101, 116]. These works have documented the dynamics of tropical moist forests and their underlying pressures within and outside protected areas, thereby establishing a solid baseline understanding of large-scale trends. However, fine-scale, spatially explicit analyses remain scarce, despite their critical importance for uncovering local mechanisms and informing targeted forest management interventions. Encouragingly, recent methodological advances now make such work increasingly feasible. Radar time-series approaches, for instance, can now detect forest degradation and disturbance at resolutions down to 100 m [109], while new algorithms such as the 3DC method allow rapid detection of deforestation events from Sentinel-1 radar data [114]. In parallel, methodological reviews and synthesis efforts have clarified the strengths and limitations of current remote sensing tools for monitoring forest degradation [70], and emerging spatially explicit approaches enable the near-real-time tracking of small-scale disturbance

drivers such as logging and fire [91]. Yet, despite this growing toolkit, such approaches have seldom been applied in African protected areas, leaving important knowledge gaps in landscapes such as the Kahuzi-Biega National Park (KBNP).

Addressing this gap is critical, as fine-scale and spatially explicit assessments of forest dynamics remain rare in African protected areas, despite their importance for conservation planning and adaptive management. Building on the globally consistent land-cover data of Vancutsem et al. [107] the present study provides one of the first detailed analyses of tropical moist forest change in the Kahuzi-Biega National Park (KBNP) landscape. By examining forest dynamics over more than three decades (1990–2023), this study contributes to a better understanding of how different change processes interact and how they are shaped by ecological context and landscape factors. Specifically, the objectives are to: (1) Map and characterise, using a “pixel of interest” approach, the principal pathways of forest change, including deforestation, degradation, regeneration, and stability, across the KBNP landscape from 1990 to 2023. (2) Assess the spatial distribution of forest states (intact, degraded, deforested, regenerating) in relation to landscape composition, fragmentation patterns, and proximity to disturbance sources. (3) Analyse how fragmentation and ecological context (altitude and anthropogenic accessibility) differ among stable, deforested, degraded, and regenerating areas, with a focus on identifying whether the most intense changes are concentrated in already fragmented and accessible zones. Following Van Cutsem et al. [107], a pixel is designated as “Undisturbed tropical forest” (UTMF) if it exhibits dense, evergreen or semi-evergreen vegetation cover and shows no evidence of disturbance throughout the study period (1990–2023). Pixels are considered “degraded” if they undergo at least one short-term disturbance (duration < 2.5 years) in forest cover during study period, as detected via remote sensing. Conversely, a pixel is classified as “deforested” when it experiences a long-term conversion (duration > 2.5 years) and remains under non-forest land use for the entirety of the study period. Finally, “regrowth” pixels are those that were deforested but subsequently entered a vegetative recovery phase.

## 2 Materials and methods

### 2.1 Study area

Kahuzi-Biega National Park is located in eastern Democratic Republic of Congo between 1° 36' and 2° 37' S latitude and 27° 33' and 28° 46' E longitude (Fig. 1). Covering 6700 km<sup>2</sup>, it extends from the Congo River basin near Itebero-Utu to its western boundary northwest of Bukavu, across three provinces: South Kivu, North Kivu, and Maniema [41, 94]. The park comprises two distinct sectors linked by a narrow ecological corridor: a high-altitude zone, whose summit is Mount Kahuzi (3308 m), and a low-altitude zone ranging from 600 to 1700 m above sea level [8, 48, 103].

The KBNP encompasses two distinct climatic zones: the lowland Guineo-Congolian tropics and the Afro-montane tropics [9]. In the lowland sector, daytime temperatures remain uniformly warm year-round, with a mean annual temperature of 20.5 °C and very high rainfall throughout the year. Two rainy seasons occur, May to June and October to December, each separated by brief dry intervals. In the montane zone, an Afro-alpine climate predominates, with nocturnal frosts occasionally affecting the summits of Kahuzi and Biega. Daytime conditions are often overcast, with intense precipitation.

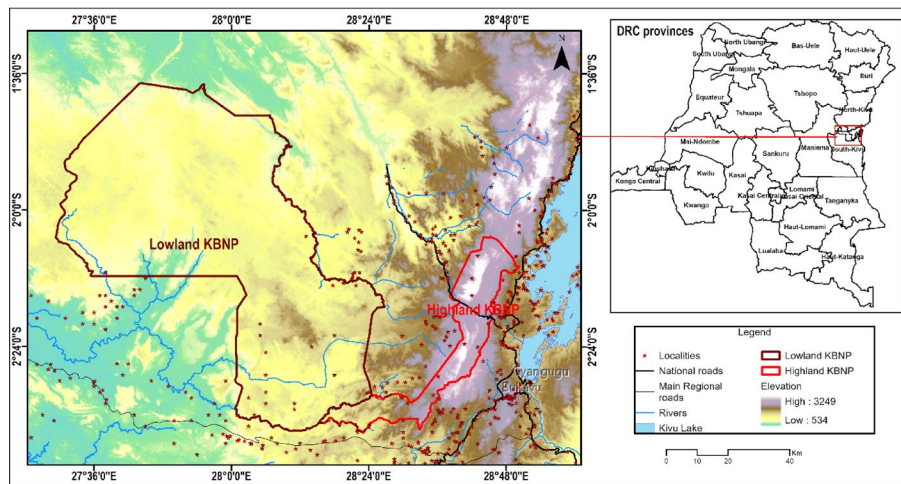


**Fig. 1** Study area comprising Kahuzi-Biega National Park and a 15 km peripheral buffer zone beyond its boundaries. The park is located in eastern Democratic Republic of Congo (DRC), spanning the provinces of North Kivu, South Kivu, and Maniema

Mean annual rainfall may reach up to 1900 mm, with a prolonged dry season from June to August and a short dry spell in February [9, 35, 63, 71].

Approximately 60% of the park remains as intact forest [80] spanning the full altitudinal gradient from 600 m to over 2600 m and encompassing all successional stages of tropical forest vegetation [48, 78, 103]. Its fauna includes 136 mammal species, notably the critically endangered eastern lowland gorilla (*Gorilla beringei graueri*) and several other threatened primates. The park is dissected by numerous waterways and traversed in the high-altitude sector by National Road 2 [48]. Human activities, such as artisanal mining, traditional trapping, rudimentary trails, and seasonal cultivation, are present in certain areas of the park [9, 93].

## 2.2 Data used

The Table 1 presents the data used to analyse the main pathways of TMF dynamics and their ecological.

## 2.3 Data analysis

### 2.3.1 Data pre-processing

- Resampling and reclassification: to ensure consistency with the spatial resolution of Landsat images and ancillary datasets, imagery from Van Cutsem et al. [107]-annual change collection, “Deforestation Year”, “Degradation Year” and “Deforestation After Degradation”—with initial spatial resolution of 29.9 m were resampled to a 30 m spatial resolution. Subsequently they were reclassified into five classes representing the main processes to which can pass the undisturbed TMF: Undisturbed tropical moist forest (UTMF), degradation, deforestation, forest regrowth, and other land-cover types. For each class, total area (relative value) and annual change rates were calculated for the period 1990–2023.
- Transition analysis: following area calculations for each process, landscape conversion dynamics were quantified using a transition matrix [11, 13]. The transitions called here “pathways” were analyzed between two time points. The year

**Table 1** Overview of datasets used to analyze tropical moist forest (TMF) dynamics and their ecological context described by the altitude and anthropogenic accessibility in Kahuzi-Biega National Park from 1990 to 2023

Dataset name	Data source	Spatial resolution	Temporal coverage	Purpose in this study
Annual Land-Use Change Collection	Vancutsem et al. [107], Forest Observations portal (projects/JRC/TMF/v1_2023/AnnualChanges)	30 m	1990–2023	Detect annual TMF change and classify into stability, degradation, deforestation, and regrowth pathways
Deforestation Year/ Degradation Year/ Deforestation after Degradation Year	Vancutsem et al. [107], Forest Observations portal (“Asset ID: projects/JRC/TMF/v1_2023/Deforestation-Year”), “Degradation Year” (Asset ID: projects/JRC/TMF/v1_2023/DegradationYear) and “Deforestation After Degradation” (Asset ID: projects/JRC/TMF/v1_2023/DegradationAfterDegradationYear)	30 m	1990–2023	Identify year of first deforestation/Degradation events and deforestation events preceded by degradation
Artisanal mining sites	(Open data—IPIS)	Point data	2023	Map proximity to mining activities
Fire occurrence points	NASA FIRMS <a href="https://firms.modaps.eosdis.nasa.gov/">https://firms.modaps.eosdis.nasa.gov/</a>	~ 375 m	2001–2023	Map proximity to fire events
Built-up area extents	Geofabrik Download Server (OpenStreetMap)	Vector polygons	2023	Map proximity to settlements
Road network	Geofabrik Download Server (OpenStreetMap)	Vector lines	2023	Map proximity to road access
Digital Elevation Model	OpenTopography—Shuttle Radar Topography Mission (SRTM GL1)	30 m	2000	Extract altitude as a physical variable

The table includes information on data sources, spatial and temporal resolution, and their specific role in identifying forest change pathways and related environmental factors

1990, which served as the baseline year, marks both the earliest data availability and the prelude to major disturbances; namely the onset of armed conflict and large-scale population displacements beginning in 1996 [50, 72]. The year 2023, which represent the end state, encompasses all landscape dynamics that occurred in the landscape since 1990. From the transition matrix 10 pathways of TMF dynamics were identified (Fig. 2).

- Selection and preprocessing of variables describing the ecological context: in addition to the primary pathways related to TMF dynamics, we incorporated altitude (a key physical parameter) and the principal drivers of TMF change previously identified by Cirezi et al.[20] in the Kahuzi-Biega landscape, namely, artisanal mining sites, built-up areas, roads, and fire-occurrence. For drivers available as vector shapefiles

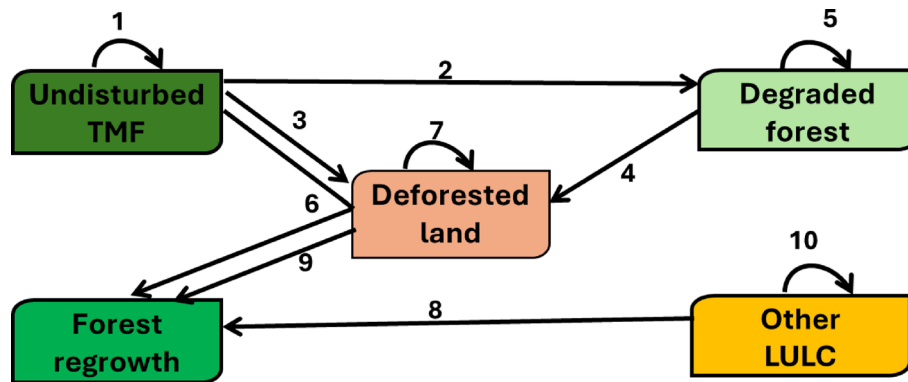


**Fig. 2** Primary transition pathways of undisturbed tropical moist forest (TMF) dynamics within the Kahuzi-Biega National Park (KBNP) landscape from 1990 to 2023. The figure illustrates major land use/land cover (LULC) changes, highlighting patterns of stability, degradation, deforestation, and regrowth across the study period

(points or lines), we generated 30 m-resolution rasters by computing Euclidean distance to represent spatial accessibility and pressure gradients [27]. Euclidean distance was chosen because it provides a continuous, quantitative approximation of proximity to potential disturbance sources, serving as a widely used proxy for anthropogenic accessibility and pressure in spatial ecological models [3, 10, 77, 108]. Approaches using Euclidean distance at 30 m resolution have effectively modelled forest change where detailed cost-distance data are unavailable [3, 77]. Following Euclidean distance computation for each variable, we assessed pairwise Pearson correlations and visualized the results using a corrplot [95]. As Euclidean distance to roads and to built-up areas were highly collinear ( $r^2 > 0.90$ ), only distance to roads was retained in the subsequent models.

- Image quality and suitability assessment: in addition to the analysis of Van Cutsem’s datas’ suitability for the KBNP landscape context carried out by Cirezi et al.[20], field inventory was conducted from July 2023 to December 2023. A total of 63 plots of 0.25 ha each [62], arranged along 1 km north-oriented transects following the disturbance gradient (“Appendix 1”), were surveyed. Within these plots, anthropogenic disturbances were recorded (presence/absence) on site. The individual plots were then overlaid to the transition matrix (1990–2023), which groups the primary land-cover dynamics, in order to document the changes observed via satellite imagery.

All preprocessing steps were performed using ArcGIS Pro 3.1.0 using the Reclassify and Raster Calculator tools.

### 2.3.2 Sampling

For each pathway of TMF dynamic (transition/stability), we randomly sampled 600 pixels of interest (POI) (200 pixels  $\times$  3 replicates), yielding a total of 6000 sampled pixels across the study landscape. Around each POI representing the focal pixel we centred a fixed square analysis window (hereafter referred to as the “landscape”) [84] and extracted its surrounding land-cover pattern. Three nested window sizes were used,  $3 \times 3$  pixels (0.0081 km<sup>2</sup>),  $9 \times 9$  pixels (0.0729 km<sup>2</sup>), and  $27 \times 27$  pixels (0.6561 km<sup>2</sup>), following the approach of Riitters et al. [85] and adapted to the study scale.

### 2.3.3 Tropical moist forest pathways characterisation

- Landscape composition and configuration analysis: for each fixed window (across all scales), we assessed landscape composition and configuration by computing the number and frequency of TMF pathways and visualising these patterns using frequency heatmaps [111]. We also calculated key spatial-structure metrics including patch density (PD), largest patch index (LPI), and edge density (ED), to quantify the degree of fragmentation and dominance of remaining forest patches [31, 68]. All metrics were computed in R 4.2.2. using the `landscapeTools` and `landscapeMetrics` packages [99]. These indicators enabled us to distinguish fine-scale landscape responses associated with each forest-transition pathway.
- Ecological context characterisation and their impact on the key processes in the landscape: environmental covariates describing the ecological context mean altitude, mean distance to fire-occurrence points, mean distance to roads, and mean distance to artisanal mining sites have been calculated for each window. The main processes include overall change (all transition types combined), deforestation, degradation, and forest regrowth. For each process, we created a binary response variable (0 for pixels not experiencing the process; 1 for pixels where the process occurred). We then fitted a logistic regression, with mean altitude and mean distances to roads, fire events, and mining sites as explanatory covariates, using a generalized linear model (GLM) with a logit link. Model fitting was conducted in R via `glm(..., family = binomial(link = "logit"))`, following McCullagh and Nelder's [67] recommendations for analyzing binary response data within the exponential-family framework.

### 2.3.4 Statistical analysis

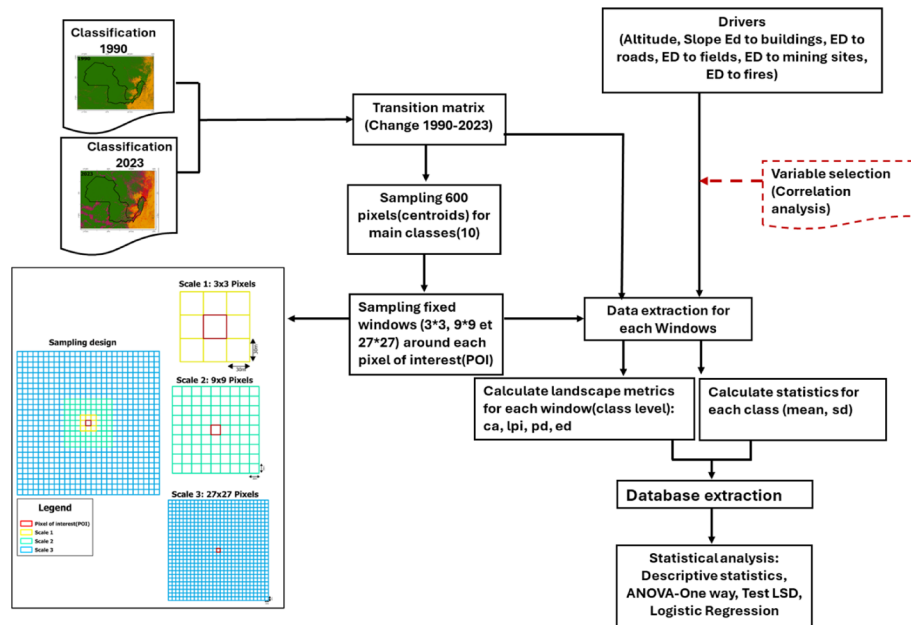
For each computed parameter, a comparative assessment across the main pathways of TMF dynamics at different window sizes was conducted. First, data were aggregated by class and scale using a summary function to estimate means and standard deviations for each factor combination [110]. Next, a one-way analysis of variance (ANOVA) was carried out to determine whether the observed differences in means among the classes were statistically significant [34]. Whenever the ANOVA indicated a significant effect ( $p < 0.05$ ), a Fisher's LSD (Least Significant Difference) post-hoc test was performed using the `LSD.test()` function from the `agricolae` package [26]. The Figure 3 summarises the full methodological workflow for sampling and data analysis.

## 3 Results

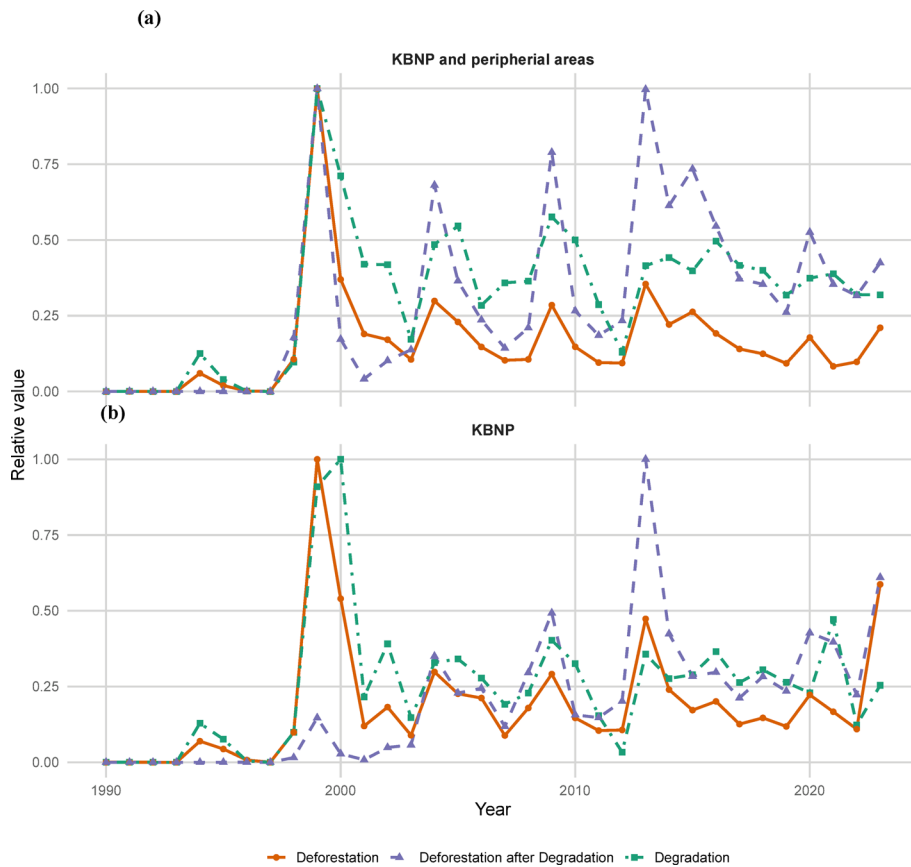
### 3.1 Annual dynamics for deforestation, degradation and deforestation following degradation

Figure 4 shows the annual dynamics of forest degradation, deforestation, and deforestation following degradation in the KBNP landscape and its peripheral areas from 1990 to 2023.

Figure 4 indicate two major peaks of disturbance during the study period, one in the late 1990s (around 1998) and another in the early 2010s (around 2013). Deforestation within KBNP is characterised by sharp but short-lived spikes, while degradation exhibits more frequent and recurrent fluctuations. Regrowth is present but remains comparatively low across the entire period. In the peripheral areas, disturbance levels are



**Fig. 3** Synthesis of the methodological workflow used to analyse the pathways of tropical moist forest (TMF) dynamics in the Kahuzi-Biega National Park (KBNP) landscape from 1990 to 2023



**Fig. 4** Annual dynamics of forest degradation, deforestation, and deforestation after degradation in KBNP and its peripheral zones (1990–2023)

generally higher and more sustained, with prolonged periods of both degradation and regrowth compared to the interior of KBNP.

### 3.2 Main pathways of TMF dynamics in the KBNP landscape

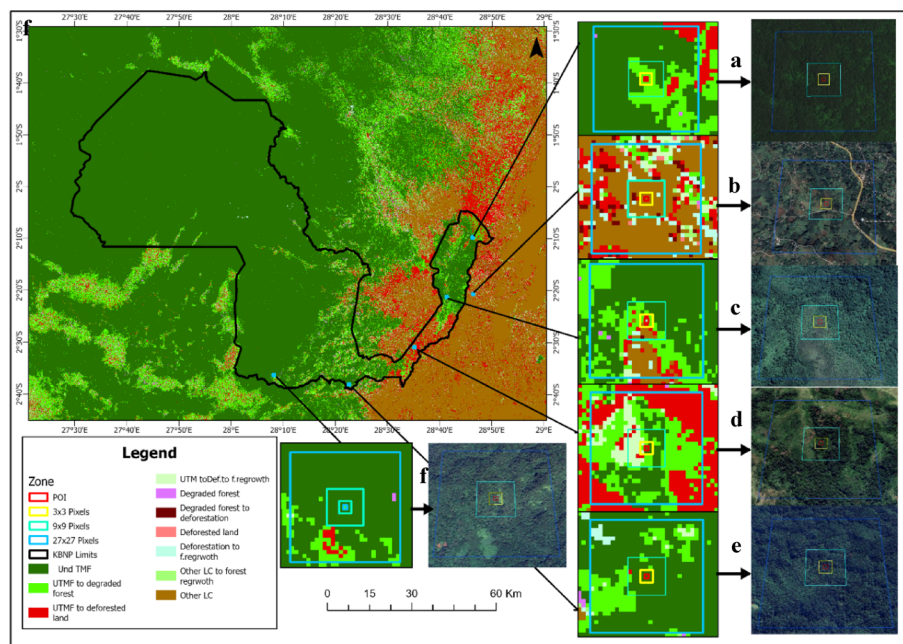
Figure 5 and Table 1 present the transition matrix of the main pathways of TMF dynamics that occurred in the Kahuzi-Biega National Park landscape from 1990 to 2023.

Figure 4 and the Table 2 show that despite the various disturbances experienced in the Kahuzi-Biega landscape, the undisturbed TMF still cover over 64.2% of the area. Between 1990 and 2023, approximately 4606.4 km<sup>2</sup> (17.2% of the landscape) of intact forest was converted—specifically, to degraded forest (2737.4 km<sup>2</sup>; 10.2%) and to non-forest land uses (deforestation: 1551.8 km<sup>2</sup>; 5.8%). A further 317.6 km<sup>2</sup> (1.18%) underwent deforestation before progressing to forest regrowth. Of the area already degraded in 1990 (201.0 km<sup>2</sup>; 0.75%), 162.8 km<sup>2</sup> (0.6%) was subsequently deforested. Conversely, 73.2 km<sup>2</sup> (0.3%) of the area initially deforested in 1990 experienced forest regrowth. Land originally classified as “Other LULC” remained unchanged throughout the study period, while all other minor transitions were associated with combinations of degradation, deforestation, and/or regrowth.

### 3.3 Image suitability assessment

Table 3 presents the accuracy assessment of disturbance detection from Landsat-derived classifications against field inventory records in the Kahuzi-Biega National Park (KBNP) landscape.

Table 3 shows that Landsat-derived classifications captured 69.8% of the disturbances observed in the KBNP landscape. All instances of deforestation and forest regrowth



**Fig. 5** Main pathways of tropical moist forest (TMF) dynamics in the Kahuzi-Biega National Park (KBNP) landscape from 1990 to 2023. The panels represent different pixel-of-interest (POI) categories: (a) undisturbed TMF → deforested land, (b) other land-use/land-cover (LULC), (c) deforested land → forest regrowth, (d) undisturbed TMF → forest regrowth, (e) undisturbed TMF, and (f) undisturbed TMF → degraded forest. Insets provide zoomed views of landscape composition and configuration across analysis window sizes; for each case, the left panel shows the transition-matrix map and the right panel the corresponding final-state (2023) image from Google Earth Pro

**Table 2** Transition matrix of tropical moist forest (TMF) dynamics within the Kahuzi-Biega National Park (KBNP) landscape from 1990 to 2023

		1990					
Transition classes		Undisturbed TMF km <sup>2</sup> (%)	Degraded forest km <sup>2</sup> (%)	Deforested land km <sup>2</sup> (%)	Forest regrowth* km <sup>2</sup> (%)	Others LULC km <sup>2</sup> (%)	Total km <sup>2</sup> (%)
2023	Undisturbed TMF km <sup>2</sup> (%)	<b>17,291.4 (64.2)</b>	0	0	0	0	17,291.4 (64.2)
	Degraded forest km <sup>2</sup> (%)	2737.3 (10.2)	<b>201.0 (0.7)</b>	0	0	0	2938.3 (10.9)
	Deforested land km <sup>2</sup> (%)	1551.7 (5.8)	162.8 (0.6)	<b>288.0 (1.1)</b>	0	0	2002.5 (7.4)
	Forest regrowth* km <sup>2</sup> (%)	317.6 (1.2)	0	73.2 (0.3)	<b>0</b>	227.9 (0.8)	618.7 (2.3)
	Other LULC km <sup>2</sup> (%)	0	0	0	0	<b>4073.8 (15.1)</b>	4073.9 (15.1)
	Total km <sup>2</sup> (%)	21,898.1 (81.3)	363.8 (1.3)	361.1 (1.3)	0	4301.8 (16.0)	<b>26,924.9 (100)</b>

Values represent the area (km<sup>2</sup>) and corresponding percentage of each land-use/land-cover (LULC) class in 2023, as a function of its state in 1990. Transition classes include: Undisturbed TMF, Degraded forest, Deforested land, Forest regrowth, and Other LULC (non-forest classes such as agriculture and settlements). \*Forest regrowth refers to areas that were previously deforested but subsequently reverted to woody vegetation cover. Percentages are expressed relative to the total study area (26,924.9 km<sup>2</sup>). The bold values on the diagonal represent stable areas.

**Table 3** Accuracy assessment of disturbance detection from Landsat classifications compared with field survey records in the Kahuzi-Biega National Park (KBNP) landscape

Pathway types identified on the image	Disturbances recorded on the ground			% Of detection on the ground	Main disturbances recorded on the ground(N)
	Absence	Presence	Total		
Degradation	8	19	27	<b>70.4</b>	Wood cutting (19), Charcoal production (11), Agriculture (5), Poaching (1), Accessibility by road (5), Human settlements (3), Livestock farming (2), Mining (2), Presence of reforestation species (1), Vegetation fires (1),
Deforestation	0	13	13	<b>100.0</b>	Charcoal production (11), Vegetation fires (9), Agriculture (8), Logging (8), Livestock farming (7), Animal tracks (7), Mining (2), Presence of reforestation species (2), Poaching (1)
Forest Regrowth	0	3	3	<b>100.0</b>	Presence of reforestation species (2), Logging (2), Charcoal production (1),
Undisturbed TMF	11	8	19	<b>42.1</b>	Wood cutting (4), Charcoal production (4), Poaching(2)
Other LULC	0	1	1	<b>100.0</b>	Agriculture(1), Wood cutting (2), Charcoal production (3)
Total	<b>19</b>	<b>44</b>	<b>63</b>	<b>69.8</b>	

The assessment was based on 63 field plots (0.25 ha each) distributed along disturbance gradients and surveyed between July and December 2023. Disturbance observations (presence/absence) were overlaid with satellite-derived classifications of undisturbed tropical moist forest (UTMF), degraded forest, deforested land, forest regrowth, and other land-use/land-cover (LULC). The values in bold represent, on the one hand, the total number of plots inventoried on the ground and, on the other hand, the percentage of detection on the ground.

detected in the imagery were confirmed by field inventories, indicating high reliability for these processes. By contrast, degradation was identified with a moderate accuracy of 70.4%, with detection rates varying according to the intensity of disturbance at each plot. However, a substantial proportion of disturbances (57.9%) occurring within areas classified as undisturbed forest, particularly small-scale or selective activities such as logging, charcoal production, and poaching, were not detected by the imagery, highlighting the limitations of medium-resolution satellite data in capturing fine-scale disturbances.

### 3.4 Class diversity around pixels of interest (POI)

The analysis of class diversity around class of interest (i.e. pixels belonging to the various pathways of dynamics) is presented in Fig. 5 at three spatial scales: (a) 3 × 3 pixels, (b) 9 × 9 pixels, and (c) 27 × 27 pixels.

Figure 6 demonstrates that the composition of land-cover classes surrounding points of interest (POIs) varies with both spatial scale and the transition pathway of tropical moist forest (TMF) dynamics, while maintaining consistent overall trends ( $\chi^2 = 1494.7$ ,  $df = 18$ ,  $p < 0.001$ ). At the 3 × 3-pixel scale (0.0081 km<sup>2</sup>), undisturbed TMF pixels are predominantly neighbored by other intact forest (85%), reflecting strong local stability, whereas degraded and deforested pixels are mainly surrounded by same-class neighbours (40% and 36%, respectively), indicating spatial clustering of disturbance. By contrast, degraded-to-deforested pixels show higher adjacency with “other LC” (29%), pointing to transitional zones where forest clearance advances into the non-forest matrix. At the 9 × 9-pixel scale (0.0729 km<sup>2</sup>), undisturbed forest remains dominant in neighbourhoods (68%) but its share decreases compared to the fine scale, while degraded and deforested classes increasingly share neighbourhoods with intact forest (20% and 9%, respectively), suggesting both encroachment risks and residual connectivity. At the 27 × 27-pixel scale (0.6561 km<sup>2</sup>), undisturbed TMF pixels retain the largest same-class share (35%), but “other LC” becomes the dominant neighbour category for nearly all disturbed classes (22–25%), highlighting the pervasiveness of non-forest surroundings at broader landscape scales. These patterns illustrate three main insights. First, intact TMF cores show strong stability locally but increasing fragmentation at broader scales, implying heightened exposure to edge effects. Second, degraded and deforested pixels cluster spatially, underlining the risk of disturbance expansion into adjacent intact forest, especially in transitional zones. Third, forest regrowth pixels are embedded in mixed neighbourhoods: when adjacent to undisturbed forest, natural recovery is more likely, but regrowth surrounded by “other LC” faces stronger constraints and may require active restoration. Overall, the growing dominance of “other LC” in larger neighbourhoods emphasises the influence of the surrounding matrix on both the persistence of intact forest and the recovery potential of disturbed areas. This scale-dependent class diversity analysis therefore provides critical context for conservation in KBNP by identifying

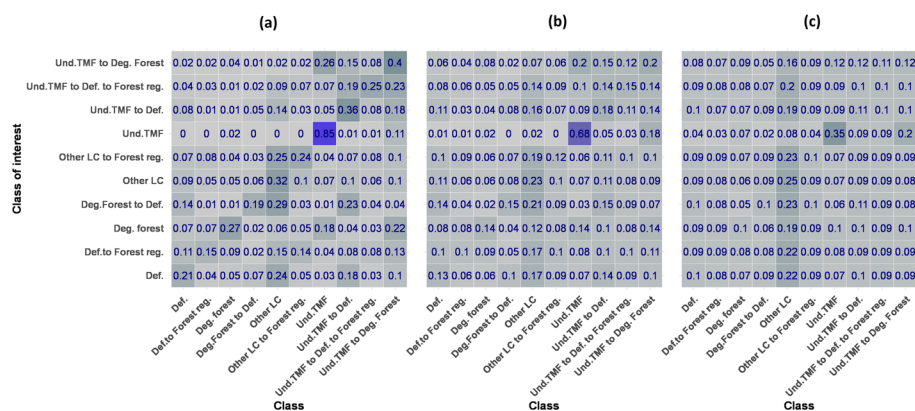


**Fig. 6** Heatmaps of class-diversity frequencies(values divided by 100) around POI in the Kahuzi-Biega National Park landscape (1990–2023) are presented at three spatial scales—3 × 3 pixels (a), 9 × 9 pixels (b), and 27 × 27 pixels (c)—with the following legend: Und. TMF: Undisturbed Tropical Moist Forest, Def.: Deforested, Deg.: degraded, Reg: Regrowth

stable cores needing protection, high-risk clusters requiring monitoring, and regrowth patches where restoration could enhance resilience.

### 3.5 Characterization of the spatial configuration and ecological context of the main pathways of TMF dynamics

#### 3.5.1 Spatial configuration of the main pathways of TMF dynamics

The Fig. 7 summarizes the spatial configuration of the landscape surrounding the pixels of interest (PIO) within the Kahuzi-Biega National Park landscape across the three analysis scales. The metrics considered indicate fragmentation levels (Edge Density [ED], Largest Patch Index [LPI], Patch Density [PD]).

The heatmap on the Fig. 7 demonstrates that the various TMF dynamics pathways exhibit significantly different spatial configurations ( $p < 0.0001$  for all indices). Across all three spatial scales, the undisturbed TMF exhibits the lowest edge density (ED) and highest largest-patch index (LPI) of all pathways, indicating large, contiguous forest patches with minimal edge effects (e.g. at  $3 \times 3$  pixels:  $ED = 27.8 \pm 51.6$  m/ha vs.  $107.4 \pm 50.7$  m/ha for “undisturbed  $\rightarrow$  degraded”;  $LPI = 85.1 \pm 28.5\%$  vs.  $38.4 \pm 27.5\%$ ). Its patch density (PD)

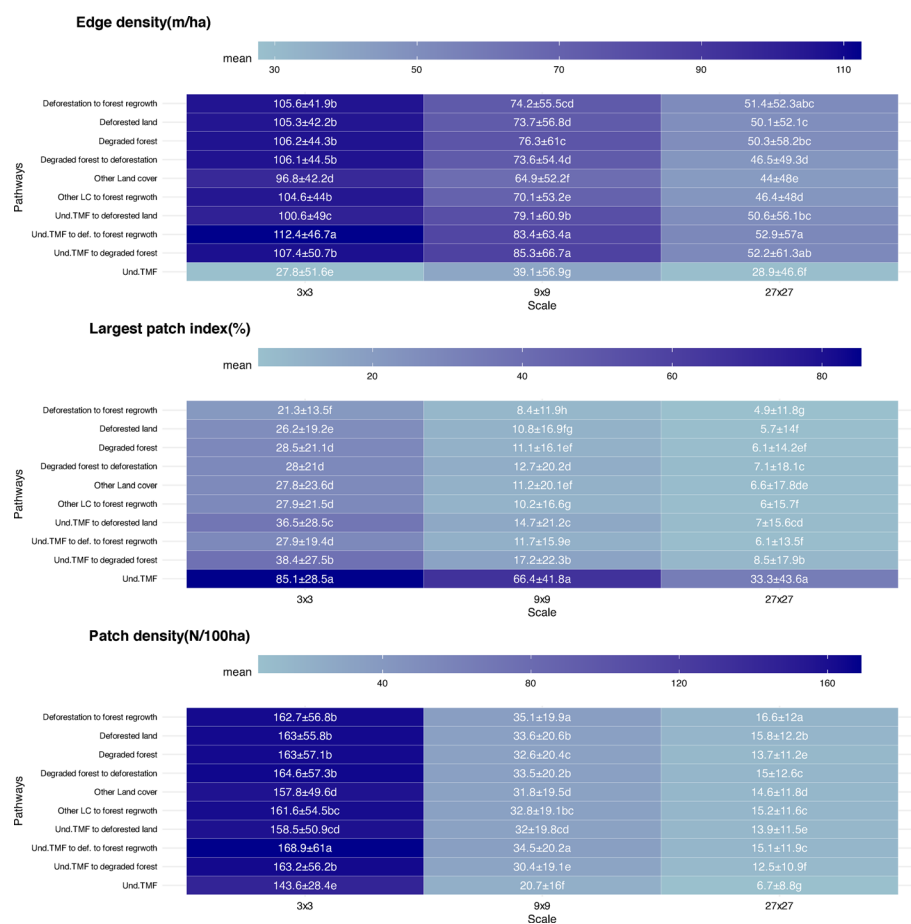


**Fig. 7** Spatial configuration metrics of the POI landscape in the Kahuzi-Biega National Park (1990–2023) calculated at three spatial scales ( $3 \times 3$ ,  $9 \times 9$ , and  $27 \times 27$  pixel windows). Metrics include edge density (m/ha), largest patch index (%), and patch density (N/100 ha). Values are expressed as mean  $\pm$  standard deviation. Letters indicate statistically homogeneous groups according to Fisher's LSD (Least Significant Difference) post hoc test ( $p < 0.05$ ) following one-way ANOVA for each metric and scale; identical letters within a column denote no significant difference between pathways, while different letters indicate significant differences

is also markedly lower at the broadest scale ( $6.7 \pm 8.8$  patches/ha at  $27 \times 27$ ), consistent with a single large patch rather than many small fragments. The other pathways of TMF dynamics (e.g. “undisturbed  $\rightarrow$  degraded,” “degraded  $\rightarrow$  deforestation”) show substantially higher ED and PD and lower LPI, reflecting more broken and irregular patch structures. As the window size increases, the absolute values of ED and PD decrease and the LPI declines, reflecting the smoothing effect of larger spatial contexts. However, the relative ranking of tracks remains consistent at all scales: undisturbed TMF always exhibits the most cohesive pattern, while mixed and degraded classes remain the most fragmented. The letters displayed in Fig. 7 represent the grouping of pathways into statistically homogeneous subsets. Pathways sharing the same letter do not differ significantly for that metric at the given scale, whereas pathways with different letters exhibit statistically significant differences. For example, at the  $3 \times 3$  scale for edge density, “deforestation to forest regrowth” ( $105.6 \pm 41.9$  m/ha, letter b) differs significantly from “undisturbed TMF” ( $85.2 \pm 51.6$  m/ha, letter e), indicating higher edge complexity in regrowth patches compared to intact forest.

### 3.5.2 Ecological context

The Fig. 8 summarizes the ecological context of the landscape surrounding the pixels of interest (POI) within the Kahuzi-Biega National Park landscape across the three analysis scales. The variables considered include the environmental parameter—here the mean altitude, and the distance to the main disturbances (mean distance to roads, mean distance to artisanal mining sites, and mean distance to fire occurrences).

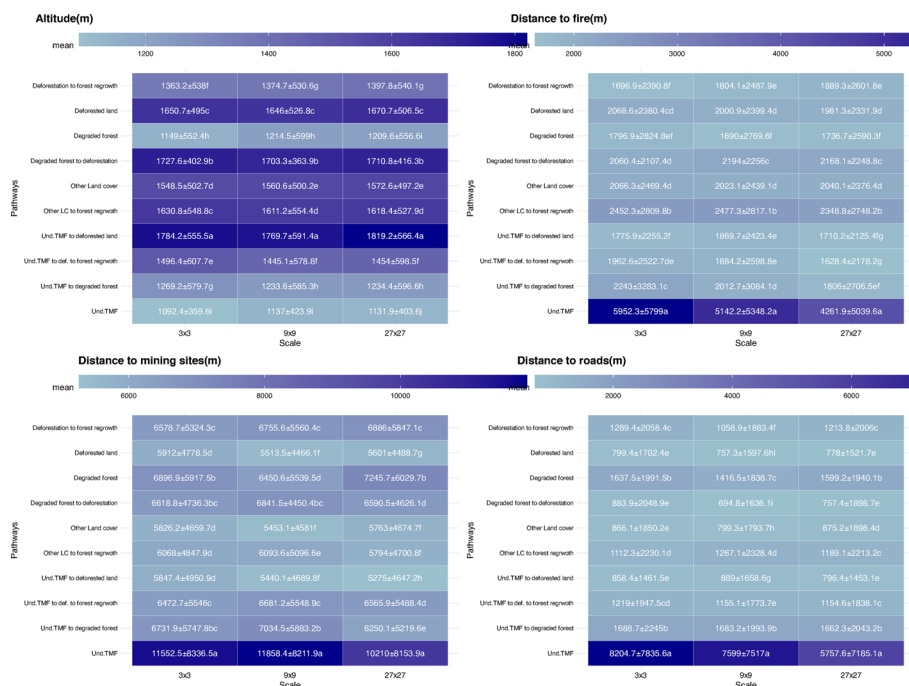


**Fig. 8** Ecological context of the POI landscape in the Kahuzi-Biega National Park (1990–2023) calculated at three spatial scales ( $3 \times 3$ ,  $9 \times 9$ , and  $27 \times 27$  pixel windows). Ecological context include altitude (m) and indicators of anthropogenic accessibility such as distance to roads(Km), distance to fires and distance to minings. Values are expressed as mean  $\pm$  standard deviation. Letters indicate statistically homogeneous groups according to Fisher’s LSD (Least Significant Difference) post hoc test ( $p < 0.05$ ) following one-way ANOVA for each metric and scale; identical letters within a column denote no significant difference between pathways, while different letters indicate significant differences

Figure 8 shows the ecological context that characterizes the landscape of the pixels of interest (POIs). Post-hoc analyses and examination of the values of the parameters associated with each pathway reveal that the undisturbed TMF pathway is statistically distinct from all other pathways. The undisturbed TMF is mainly located at lower altitudes, which likely reflects the fact that much of the study area lies at lower altitude and further away from disturbances such as fires ( $5.9 \pm 5.8$  m), mining sites ( $11.5 \pm 8.3$  m) and roads ( $8.2 \pm 7.8$  m). This highlights its relative remoteness and inaccessibility. Pathways of degradation and deforestation are much closer to roads and fires (e.g., “intact  $\rightarrow$  degraded” Distance to fire =  $2.2 \pm 3.2$  m; Distance to roads =  $1.7 \pm 2.2$  m), highlighting the role of access and sources of disturbance in the evolution of TMFs. Overall, these results demonstrate that the persistence of intact forests in Kahuzi-Biega is strongly linked to lower altitude, greater isolation from roads and fires, and a cohesive plot structure. In contrast, degradation and deforestation occur in more accessible areas at higher altitudes.

### 3.5.3 Influence of ecological context on main processes in the Kahuzi-Biega National Park landscape

The regression results in the Table 4 reveal that the main drivers of forest dynamics in the study area are altitude, proximity to roads, and fire disturbances, with mining exerting only a limited influence. Deforestation was strongly associated with higher altitudes (OR 2.22–2.49,  $p < 0.001$ ) and occurred preferentially near roads (OR 0.89–0.91,  $p < 0.001$ ) and fire-affected zones (OR 0.91–0.93,  $p < 0.001$ ), while mining showed no significant relationship ( $p > 0.58$ ). In contrast, degradation was concentrated at lower altitudes (OR 0.27–0.30,  $p < 0.001$ ) and was consistently facilitated by road accessibility (OR 0.91–0.92,  $p < 0.001$ ), with a modest but significant influence of mining activities (OR 1.01–1.02,  $p = 0.031$ –0.039), whereas fire played only a marginal role ( $p = 0.063$  at  $9 \times 9$  scale). When considering overall forest dynamics (deforestation and degradation combined), the effects of altitude (OR 1.16–1.34,  $p \leq 0.014$ ), roads (OR 0.91–0.93,  $p < 0.001$ ), and fire (OR 0.92–0.93,  $p < 0.001$ ) remained dominant, confirming the critical role of accessibility and disturbance in shaping forest transitions, with mining exerting a weak effect at the  $9 \times 9$  scale ( $p = 0.035$ ). Patterns of forest regrowth were more variable, but regrowth tended to be suppressed near roads (OR 0.92–0.94,  $p < 0.001$ ) and fire-affected areas (OR 0.92–0.95,  $p \leq 0.002$ ) and, at intermediate scales, at higher altitudes (OR 0.78,  $p < 0.001$ ), while weak positive associations with mining sites were detected (OR  $\approx 1.01$ ,  $p = 0.045$ ; marginal at  $p = 0.068$ ).

## 4 Discussion

### 4.1 Methodological approach and study limitations

Degradation and loss of undisturbed tropical moist forest pose critical challenges for ecosystem functioning, climate regulation, and biodiversity [37, 92]. These forests, characterized by very low fragmentation and high species richness compared to disturbed areas, play a key role in maintaining global ecological balance [30]. In order to understand the local dynamics that support its variability in time and space, we characterise the pathways of the Tropical Moist Forest (TMF) dynamics within the Kahuzi-Biega National Park landscape, one of the DRC’s key protected areas, whose conservation second target is its contiguous, biodiversity-rich intact moist forest block [48]. We adapted the fragmentation-pattern methodology of Riitters et al. [85] to the local context by using

**Table 4** Logistic regression results (odds ratios with 95% confidence intervals and *p*-values) for the main drivers of forest processes across three spatial scales (3 × 3, 9 × 9, and 27 × 27 windows)

Processes	Predictors	Scale 1(3 × 3)			Scale 2(9 × 9)			Scale 3(27 × 27)		
		OR (95% CI)	<i>p</i> -value	Sig	OR (95% CI)	<i>p</i> -value	Sig	OR (95% CI)	<i>p</i> -value	Sig
Dynamics	Altitude (km)	1.34 (1.21–1.48)	< 0.001	***	1.16 (1.03–1.30)	<i>0.014</i>	*	1.26 (1.14–1.39)	< 0.001	***
Dynamics	Proximity to fire (km)	0.93 (0.91–0.95)	< 0.001	***	0.93 (0.91–0.95)	< 0.001	***	0.92 (0.90–0.94)	< 0.001	***
Dynamics	Proximity to mines (km)	1.00 (0.99–1.01)	0.939		1.01 (1.00–1.03)	<i>0.035</i>	*	1.00 (0.99–1.01)	<i>0.691</i>	
Dynamics	Proximity to roads (km)	0.92 (0.90–0.95)	< 0.001	***	0.91 (0.88–0.93)	< 0.001	***	0.93 (0.91–0.95)	< 0.001	***
Deforestation	Altitude (km)	2.49 (2.23–2.77)	< 0.001	***	2.22 (1.95–2.52)	< 0.001	***	2.44 (2.18–2.73)	< 0.001	***
Deforestation	Proximity to fire (km)	0.93 (0.90–0.95)	< 0.001	***	0.91 (0.89–0.94)	< 0.001	***	0.91 (0.88–0.93)	< 0.001	***
Deforestation	Proximity to mines (km)	1.00 (0.99–1.01)	0.806		1.00 (0.98–1.01)	<i>0.726</i>		1.00 (0.98–1.01)	<i>0.581</i>	
Deforestation	Proximity to roads (km)	0.91 (0.88–0.93)	< 0.001	***	0.90 (0.87–0.93)	< 0.001	***	0.89 (0.86–0.92)	< 0.001	***
Degradation	Altitude (km)	0.27 (0.23–0.31)	< 0.001	***	0.28 (0.23–0.33)	< 0.001	***	0.30 (0.26–0.35)	< 0.001	***
Degradation	Proximity to fire (km)	1.01 (0.99–1.04)	0.281		1.03 (1.00–1.06)	<i>0.063</i>	†	1.01 (0.99–1.04)	<i>0.277</i>	
Degradation	Proximity to mines (km)	1.01 (1.00–1.03)	0.036	*	1.02 (1.00–1.03)	<i>0.031</i>	*	1.01 (1.00–1.03)	<i>0.039</i>	*
Degradation	Proximity to roads (km)	0.92 (0.89–0.94)	< 0.001	***	0.91 (0.88–0.94)	< 0.001	***	0.92 (0.89–0.94)	< 0.001	***
Forest regrowth	Altitude (km)	0.94 (0.84–1.05)	0.288		0.78 (0.68–0.90)	< 0.001	***	0.89 (0.79–1.00)	<i>0.052</i>	†
Forest regrowth	Proximity to fire (km)	0.94 (0.91–0.96)	< 0.001	***	0.95 (0.92–0.98)	<i>0.002</i>	**	0.92 (0.89–0.95)	< 0.001	***
Forest regrowth	Proximity to mines (km)	1.00 (0.99–1.01)	0.770		1.01 (1.00–1.03)	<i>0.045</i>	*	1.01 (1.00–1.02)	<i>0.068</i>	†
Forest regrowth	Proximity to roads (km)	0.94 (0.91–0.97)	< 0.001	***	0.92 (0.88–0.95)	< 0.001	***	0.94 (0.92–0.97)	< 0.001	***

Significant associations are indicated at  $p < 0.05$  (\*),  $p < 0.01$  (\*\*),  $p < 0.001$  (\*\*\*), and marginal trends at  $p < 0.10$  (†). Predictors include altitude (km), proximity to fire (km), proximity to mines (km), and proximity to roads (km). Outcomes modelled are deforestation, degradation, overall forest dynamics, and forest regrowth. The values in italic represent *p*-values.

Landsat imagery classified by Van Cutsem [107]. Consistent with [31], we treat fragmentation as a spatial pattern, evidenced by increases in patch number and decreases in patch size, rather than as a process. Unlike the moving-window approach of Riitters et al. [84] and Riitters et al. [85], which considered only forest pixels, our analysis samples fixed windows across the main pathways of change both inside and around the park. This design enables the delineation of the distinctive characteristics of each pathway and to model the ecological context (described by altitude and accessibility to anthropogenic drivers) that facilitate their occurrence.

In addition to evaluating the suitability of the Van Cutsem's et al. [107] classified images for analysing landscape dynamics in the KBNP [20], we performed field inventories to assess their capacity to capture spatio-temporal changes affecting the undisturbed TMF within the KBNP tropical landscape. Inventory results indicate that these images capture approximately 100% of deforestation events, whereas it captures only 70.4% of degradation in the KBNP landscape. Several methodological limitations help explain this discrepancy. First, although the Landsat-derived Van Cutsem et al. [107] dataset offers consistent temporal coverage and robust detection of deforestation, its medium spatial resolution (30 m) constrains the ability to identify fine-scale degradation processes, particularly those involving partial canopy loss, understory disturbance, or selective extraction in heterogeneous forest stands [7, 16, 86]. Second, persistent cloud cover in the study area limits the number of usable optical scenes per year, which may result in temporal gaps or delayed detection of rapid disturbances [46]. Third, the use of Euclidean distance to anthropogenic features as a proxy for accessibility does not account for actual travel time, topographic barriers, or seasonal variability in access, potentially underestimating the influence of human pressure in certain areas [58, 107]. Fourth, the fixed window sizes (3×3, 9×9, and 27×27 pixels) provide scale-sensitive fragmentation metrics but may not capture all relevant landscape processes occurring at scales larger or smaller than those analysed [31, 85]. Finally, field validation was necessarily constrained by security concerns and logistical limitations, which restricted our ability to sample certain disturbance types and areas [17, 72]. Collectively, these factors may introduce uncertainty into the magnitude and spatial distribution of the detected pathways, and results should therefore be interpreted as conservative estimates of actual TMF change.

#### **4.2 Pathways of TMF dynamics: spatial pattern and ecological context characterisation**

The transition matrix indicates that Kahuzi-Biega National Park landscape retains 64.2% of its undisturbed tropical moist forest (UTMF), despite measurable deforestation and degradation, with pronounced peaks around 1998 and 2013 coinciding with intense and post-armed conflict periods marked by civilian and military incursions [20, 48, 93, 105]. These findings underscore the park's intrinsic resilience, particularly in remote and less accessible zones, and are consistent with global evidence that protected areas substantially curb deforestation and degradation [25, 57, 69]. Across the KBNP landscape, the main process of change is the degradation of formerly undisturbed TMF, followed by direct deforestation. This sequence, which consists of subtle degradation preceding the clearing of parcels, is regularly observed in Amazonian and Congo Basin forests [14, 39, 64, 88] and has greater impacts on biodiversity and carbon storage than deforestation alone [83, 113, 115]. The recurrence of degradation highlights ongoing selective logging,

charcoal production, and other small-scale disturbances, while regrowth dynamics suggest that natural recovery occurs but remains limited in both magnitude and spatial extent, particularly near non-forest areas or under continued anthropogenic pressure. The stronger and more persistent disturbance signals in peripheral zones further emphasise the influence of accessibility and the weaker protection status outside the park boundaries.

The scale-sensitive analysis of class composition provides important insights into forest stability, transition risk, and recovery potential in the KBNP landscape. It reveals that intact forest cores, though still present, are increasingly embedded in heterogeneous surroundings where edge effects and human pressure heighten vulnerability [56, 73]. The spatial clustering of degraded and deforested pixels highlights high-risk zones where disturbances may expand if unmitigated [22, 44], while the distribution of regrowth underscores contrasting recovery trajectories depending on the condition of the surrounding matrix. Regrowth adjacent to intact forest is more likely to recover naturally [19], whereas patches bordered by non-forest land covers may require active restoration [6]. These patterns demonstrate that fragmentation is not only scale-dependent but also critical for identifying priority areas where protection should be reinforced, monitoring intensified, and restoration targeted [5, 82, 85]. By linking neighbourhood composition to stability, disturbance expansion, and recovery potential, this analysis strengthens the relevance of fragmentation.

Across all spatial scales, undisturbed tropical moist forests (TMF) consistently show minimal fragmentation, low edge and patch densities and high largest-patch indices, and occur in remote settings at lower altitude (much of the study area lies at lower altitude), distant from roads, fires, and mining [80]. This isolation underscores landscape configuration's role in bolstering forest resilience [76] and echoes findings that intact TMF persist in areas with limited human access [42, 101]. In contrast, pixels associated with deforestation, degradation, and regrowth share a fragmented signature, high edge and patch densities, low largest-patch indices, and lie at higher altitude near disturbance sources (roads, mining, fires). These patterns reflect the coupling of fragmentation with anthropogenic pressure and the influence of infrastructure on advancing deforestation fronts [59, 98, 101].

Logistic-regression models reveal that altitude and proximity to roads and fires increase the probability of any land-cover change. Roads facilitate deforestation by opening remote areas to logging, mining, and agriculture [24, 54], while fire often precipitates degradation [21, 106]. Conversely, regrowth is most common at lower altitudes and further from roads and burn sites, likely driven by natural recolonization or agricultural-land abandonment under favorable ecological conditions.

#### **4.3 Implications for conservation**

The findings of this study provide a clear picture of how deforestation, degradation, and regrowth unfold in and around Kahuzi-Biega National Park landscape, highlighting both the persistence of intact cores and the pressures acting on forest edges. Persistent cloud cover and security constraints limit the effectiveness of optical satellite monitoring and field inventories, but several strategies can help overcome these challenges. First, integrating freely available medium-resolution imagery with higher-resolution satellite data would improve the detection of fine-scale degradation processes. Second,

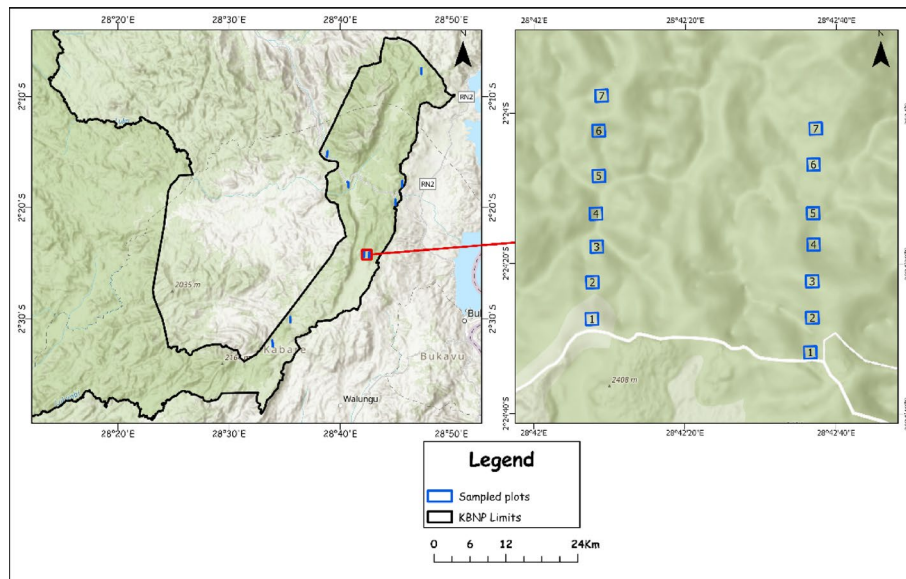
strengthening field-based monitoring through partnerships with local communities can increase data availability in areas where access is otherwise restricted. Third, combining satellite observations with systematic ground validation can improve the accuracy of disturbance detection and help differentiate between temporary and permanent changes. Fourth, building local technical capacity for image analysis and monitoring can ensure continuity and sustainability of observation efforts, while enhancing trust between park managers and communities. Finally, linking monitoring outputs to targeted conservation actions, such as reinforcing protection in high-risk zones, supporting restoration in regrowth areas with low recovery potential, and managing edge effects around intact cores, would translate monitoring data into practical management responses. Together, these measures address the current shortcomings and create a stronger foundation for adaptive forest management in the park and beyond.

## 5 Conclusion

This study applied a scale-sensitive approach, integrating Landsat-derived classifications (1990–2023) with targeted field inventories, to analyse tropical moist forest (TMF) dynamics in Kahuzi-Biega National Park (KBNP). A transition matrix quantified the main change pathways and characterised their spatial structure and ecological context at  $3 \times 3$ ,  $9 \times 9$ , and  $27 \times 27$ -pixel scales. Results show a ~23% loss of undisturbed TMF, driven mainly by degradation (10.17%) and deforestation (5.76%), with regrowth following deforestation accounting for 1.18%. Undisturbed forests consistently exhibited low fragmentation, large homogeneous patches, and greater distance from disturbance sources, underscoring their role as the ecological backbone of the park. However, degradation often precedes clear-cutting in accessible zones, highlighting the need for targeted management. The spatially explicit datasets generated here can guide prioritisation of high-risk areas for monitoring and inform interventions such as livelihood diversification in buffer zones, stricter regulation of infrastructure expansion, and restoration of degraded sites. Safeguarding KBNP's intact forests is critical for biodiversity conservation and climate regulation. Future research should combine high-resolution remote sensing with ground inventories to assess disturbance impacts on forest composition and structure, enabling adaptive and evidence-based conservation strategies.

## Appendix 1

This map shows the location of the inventory plots in Kahuzi-Biega National Park. Data was collected from 0.25-hectare plots arranged along 1-km transects oriented northward and following the disturbance gradient. There are a total of 63 plots spread over nine transects.



#### Author contributions

All authors contributed to the study conception and design. Conceptualization and design of the study was done by NCC, JB and J-FB, Material preparation, data collection and analysis were performed by NCC and YM. The first draft of the manuscript was written by NCC and all authors reviewed and edited previous versions of the manuscript. All authors read and approved the final manuscript.

#### Funding

The authors gratefully acknowledge the financial support granted ENABEL's (Belgian Development Agency) project for capacity building through the award of grants (PRECOB) in the Democratic Republic of Congo.

#### Data availability

The datasets generated during and/or analyzed during the study are available from the corresponding author on reasonable request.

#### Declarations

##### Ethics approval and consent to participate

Not applicable.

##### Consent for publication

Not applicable.

##### Competing interests

The authors declare no competing interests.

Received: 17 June 2025 / Accepted: 6 October 2025

Published online: 21 October 2025

#### References

1. Abernethy K, Maisels F, White LJT. Environmental Issues in Central Africa. *Annu Rev Environ Resour.* 2016;41:1–33. <https://doi.org/10.1146/annurev-environ-110615-085415>.
2. Achard F, Beuchle R, Mayaux P, et al. Determination of tropical deforestation rates and related carbon losses from 1990 to 2010. *Glob Chang Biol.* 2014;20:2540–54. <https://doi.org/10.1111/gcb.12605>.
3. Ahmed SE, Lees AC, Moura NG, et al. Road networks predict human influence on Amazonian bird communities. *Proc R Soc Lond B Biol Sci.* 2014;281:20141742. <https://doi.org/10.1098/rspb.2014.1742>.
4. Allan JR, Venter O, Maxwell S, et al. Recent increases in human pressure and forest loss threaten many Natural World Heritage Sites. *Biol Conserv.* 2017;206:47–55. <https://doi.org/10.1016/j.biocon.2016.12.011>.
5. Arroyo-Rodríguez V, Fahrig L. Why is a landscape perspective important in studies of primates? *Am J Primatol.* 2014;76:901–9. <https://doi.org/10.1002/ajp.22282>.
6. Arroyo-Rodríguez V, Melo FPL, Martínez-Ramos M, et al. Multiple successional pathways in human-modified tropical landscapes: new insights from forest succession, forest fragmentation and landscape ecology research. *Biol Rev.* 2017;92:326–40. <https://doi.org/10.1111/brv.12231>.
7. Asner GP. Automated mapping of tropical deforestation and forest degradation: CLASlite. *J Appl Remote Sens.* 2009;3:033543. <https://doi.org/10.1117/1.3223675>.
8. Aveling C. Le patrimoine mondial dans le Bassin du Congo, Unesco. 2010.

9. Balezi AZ. Taxonomie et écologie des Hymenochaetales dans les forêts de montagne de l'Est de la République Démocratique du Congo. Le cas du Parc National de Kahuzi-Biega. Thèse de doctorat, Université Catholique de Louvain. 2012.
10. Barber CP, Cochrane MA, Souza CM, Laurance WF. Roads, deforestation, and the mitigating effect of protected areas in the Amazon. *Biol Conserv*. 2014;177:203–9. <https://doi.org/10.1016/j.biocon.2014.07.004>.
11. Barima YS. Dynamique, fragmentation et diversité végétale des paysages forestiers en milieux de transition forêt-savane dans le Département de Tanda (Côte d'Ivoire). Université Libre de Bruxelles. 2009.
12. Bebbler DP, Butt N. Tropical protected areas reduced deforestation carbon emissions by one third from 2000–2012. *Sci Rep*. 2017. <https://doi.org/10.1038/s41598-017-14467-w>.
13. Bogaert J, Barima YSS, Ji J, et al. A methodological framework to quantify anthropogenic effects on landscape patterns. 2011. p. 141–167.
14. Bourgoïn C, Ceccherini G, Girardello M, et al. Human degradation of tropical moist forests is greater than previously estimated. *Nature*. 2024;631:570–6. <https://doi.org/10.1038/s41586-024-07629-0>.
15. Bruner AG, Gullison RE, Rice RE, da Fonseca GAB. Effectiveness of parks in protecting tropical biodiversity. *Science*. 2001;291:125–8.
16. Bullock EL, Woodcock CE, Olofsson P. Monitoring tropical forest degradation using spectral unmixing and Landsat time series analysis. *Remote Sens Environ*. 2020. <https://doi.org/10.1016/j.rse.2018.11.011>.
17. Busane RM, Kaganda M, Sheria N, et al. Analyses des dynamiques des conflits autour du PNKB. 2021.
18. Cabral AIR, Saito C, Pereira H, Laques AE. Deforestation pattern dynamics in protected areas of the Brazilian Legal Amazon using remote sensing data. *Appl Geogr*. 2018;100:101–15. <https://doi.org/10.1016/j.apgeog.2018.10.003>.
19. Chazdon RL. Second growth. Chicago: University of Chicago Press; 2014.
20. Cirezi NC, Bastin JF, Mugumaarhahama Y, et al. Analyzing drivers of tropical moist forest dynamics in the Kahuzi-Biega National Park Landscape, Eastern Democratic Republic of Congo from 1990 to 2022. *Land (Basel)*. 2025. <https://doi.org/10.3390/land14010049>.
21. Cirezi NC, Bastin JF, Tshibusu E, et al. Contribution of 'human induced fires' to forest and savanna land conversion dynamics in the Luki Biosphere Reserve landscape, western Democratic Republic of Congo. *Int J Remote Sens*. 2022;43:6406–29. <https://doi.org/10.1080/01431161.2022.2138622>.
22. Cochrane MA, Laurance WF. Synergisms among fire, land use, and climate change in the Amazon. *AMBIO J Hum Environ*. 2008;37:522–7. <https://doi.org/10.1579/0044-7447-37.7.522>.
23. Contino F. Rapport sur l'observation de la zone tampon du PNKB. 1996.
24. Damania R, Russ J, Wheeler D, Barra AF. The road to growth: measuring the tradeoffs between economic growth and ecological destruction. *World Dev*. 2018;101:351–76. <https://doi.org/10.1016/j.worlddev.2017.06.001>.
25. Damnyag L, Saastamoinen O, Blay D, et al. Sustaining protected areas: identifying and controlling deforestation and forest degradation drivers in the Ankasa Conservation Area, Ghana. *Biol Conserv*. 2013;165:86–94. <https://doi.org/10.1016/j.biocon.2013.05.024>.
26. de Mendiburu F. *Agricolae: Statistical Procedures for Agricultural Research*. 2023.
27. Dokmanic I, Parhizkar R, Ranieri J, Vetterli M. Euclidean distance matrices: essential theory, algorithms, and applications. *IEEE Signal Process Mag*. 2015;32:12–30. <https://doi.org/10.1109/MSP.2015.2398954>.
28. Dudley N. Lignes directrices pour l'application des catégories de gestion aux aires protégées. Gland: UICN; 2008.
29. Dupuis C, Lejeune P, Michez A, Fayolle A. How can remote sensing help monitor tropical moist forest degradation?—a systematic review. *Remote Sens (Basel)*. 2020;12:1087. <https://doi.org/10.3390/rs12071087>.
30. Edwards DP, Larsen TH, Docherty TDS, et al. Degraded lands worth protecting: the biological importance of Southeast Asia's repeatedly logged forests. *Proc R Soc Lond B Biol Sci*. 2011;278:82–90.
31. Fahrig L. Effects of habitat fragmentation on biodiversity. *Annu Rev Ecol Evol Syst*. 2003;34:487–515.
32. FAO. La situation des forêts dans le bassin amazonien, le bassin du Congo et l'Asie du Sud-Est. Rome. 2011.
33. FAO, UNEP. La situation des forêts du monde 2020. Forêts, biodiversité et activité humaine. FAO and UNEP. 2020.
34. Field A, Miles J, Field Z. *Discovering statistics using R*. London: SAGE Publications, Inc; 2012.
35. Fischer E, Dieterlen F, Hinkel H, et al. Die Vegetation des Parc National de Kahuzi-Biega, Sud-Kivu, Zaire mit Beiträgen von. 1993.
36. Foley JA, Asner GP, Costa MH, et al. Amazonia revealed: forest degradation and loss of ecosystem goods and services in the Amazon basin. *Front Ecol Environ*. 2007;5:25–32. [https://doi.org/10.1890/1540-9295\(2007\)5\[25:ARFDAL\]2.0.CO;2](https://doi.org/10.1890/1540-9295(2007)5[25:ARFDAL]2.0.CO;2).
37. Geist HJ, Lambin FE. Proximate causes and underlying driving forces of tropical deforestation. *Bioscience*. 2002;52:143–50.
38. Gibson L, Lee TM, Koh LP, et al. Primary forests are irreplaceable for sustaining tropical biodiversity. *Nature*. 2011;478:378–81. <https://doi.org/10.1038/nature10425>.
39. Grainger A. Constraints on modelling the deforestation and degradation of tropical open woodlands. *Glob Ecol Biogeogr*. 1999;8:179–90. <https://doi.org/10.1046/j.1466-822X.1999.00135.x>.
40. Grantham HS, Shapiro A, Bonfils D, et al. Spatial priorities for conserving the most intact biodiverse forests within Central Africa. 2020. *Environ Res Lett*. <https://doi.org/10.1088/1748-9326/ab9fae>.
41. Hall LS, Krausman PR, Morrison ML. Plea for standard terminology: The habitat concept and a plea for standard terminology. *Key words Peer refereed. Wildlife Society Bulletin*. 1997.
42. Hansen MC, Potapov PV, Moore R, et al. High-resolution global maps of 21st-century forest cover change. *Science*. 2013;342:850–3. <https://doi.org/10.1126/science.1244693>.
43. Haurez B, Dainou K, Vermeulen C, et al. A look at intact forest landscapes (IFLs) and their relevance in Central African forest policy. *For Policy Econ*. 2017;80:192–9. <https://doi.org/10.1016/j.forpol.2017.03.021>.
44. Heilman GE Jr, Stritholt JR, Slosser NC, Dellasala DA. Forest fragmentation of the conterminous United States: assessing forest intactness through road density and spatial characteristics. *Bioscience*. 2002;52:411–22.
45. Heino M, Kumm M, Makkonen M, et al. Forest loss in protected areas and intact forest landscapes: a global analysis. 2015. *PLoS ONE*. <https://doi.org/10.1371/journal.pone.0138918>.
46. Hirschmugl M, Gallaun H, Dees M, et al. Methods for mapping forest disturbance and degradation from optical earth observation data: a review. *Curr Forestry Rep*. 2017;3:32–45. <https://doi.org/10.1007/s40725-017-0047-2>.
47. Hosonuma N, Herold M, De Sy V, et al. An assessment of deforestation and forest degradation drivers in developing countries. *Environ Res Lett*. 2012;7:4009.
48. ICCN-KBNP. Plan général de gestion 2009–2019: Parc national de Kahuzi-Biega. 2010.

49. Ickowitz A, Slayback D, Asanzi P, Nasi R. Agriculture and deforestation in the Democratic Republic of the Congo: A synthesis of the current state of knowledge. Center for International Forestry Research (CIFOR). 2015.
50. Iyomi B. Parc National de Kahuzi Biega (PNKB). Fact Sheet PNKB 2. 2005.
51. Kabonyi C, Salmon M, Roche E. Le Parc National de Kahuzi - Biega (R. D. Congo), patrimoine en péril? Le secteur «Haute Altitude», situation et perspectives. *Geo Eco Trop*. 2011;35:1–8.
52. Karsenty A. Géopolitique des forêts d'Afrique centrale. *Herodote (La Découverte)*. 2020;179:108–29.
53. Kissinger G, Herold M, De Sy V. Drivers of deforestation and forest degradation: a synthesis report for REDD+ policymakers. Canada. 2012.
54. Kleinschroth F, Laporte N, Laurance WF, et al. Road expansion and persistence in forests of the Congo Basin. *Nat Sustain*. 2019;2:628–34. <https://doi.org/10.1038/s41893-019-0310-6>.
55. Ladewig M, Angelsen A, Masolele RN, Chervier C. Deforestation triggered by artisanal mining in eastern Democratic Republic of the Congo. *Nat Sustain*. 2024. <https://doi.org/10.1038/s41893-024-01421-8>.
56. Laurance WF, Camargo JLC, Luizão RCC, et al. The fate of Amazonian forest fragments: a 32-year investigation. *Biol Conserv*. 2011;144:56–67. <https://doi.org/10.1016/j.biocon.2010.09.021>.
57. Laurance WF, Carolina Useche D, Rendeiro J, et al. Averting biodiversity collapse in tropical forest protected areas. *Nature*. 2012;489:290–4. <https://doi.org/10.1038/nature11318>.
58. Laurance WF, Clements GR, Sloan S, et al. Erratum: corrigendum: a global strategy for road building. *Nature*. 2014;514:262–262. <https://doi.org/10.1038/nature13876>.
59. Laurance WF, Nascimento HEM, Laurance SG, et al. Habitat fragmentation, variable edge effects, and the landscape-divergence hypothesis. *PLoS ONE*. 2007. <https://doi.org/10.1371/journal.pone.0001017>.
60. Lewis SL, Edwards DP, Galbraith D. Increasing human dominance of tropical forests. *Science*. 2015;349:827–32.
61. Lhoest S. Biodiversity and ecosystem services in tropical forests: the role of forest allocations in the Dja area, Cameroon. 2020.
62. Mangaza L, Makana J-R, Hubau W, et al. Impacts du changement d'utilisation des terres sur la biomasse et la diversité dans le paysage forestier de la réserve de biosphère de Yangambi en République démocratique du Congo. *Bois et Forêts des Tropiques* 59–71. 2022.
63. Masumbuko NC. Écologie de *Sericostachys Scandens*, liane envahissante dans les forêts de montagne du Parc National de Kahuzi-Biega, République Démocratique du Congo. Université Libre de Bruxelles. 2011.
64. Matricardi EAT, Skole DL, Costa OB, et al. Long-term forest degradation surpasses deforestation in the Brazilian Amazon. *Science*. 2020;369:1378–82. <https://doi.org/10.1126/science.abb3021>.
65. Mayaux P, Gond V, Massart M, et al. Evolution du couvert forestier du bassin du Congo mesurée par télédétection spatiale. *Bois et forêts des tropiques*. 2003;277:45–52.
66. Mayaux P, Pekel JF, Desclée B, et al. State and evolution of the African rainforests between 1990 and 2010. *Philos Trans R Soc B Biol Sci*. 2013. <https://doi.org/10.1098/rstb.2012.0300>.
67. McCullagh P, Nelder JA. Generalized linear models. London: Routledge; 2019.
68. McGarigal K, Cushman S, Ene E. FRAGSTATS v4: Spatial Pattern Analysis Program for Categorical and Continuous Maps. 2012.
69. McNicol G, Fluet-Chouinard E, Ouyang Z, et al. Upscaling wetland methane emissions from the FLUXNET?CH4 eddy covariance network (UpCH4 v10): Model development, network assessment, and budget comparison. *AGU Adv* 4. 2023.
70. Mitchell AL, Rosenqvist A, Mora B. Current remote sensing approaches to monitoring forest degradation in support of countries measurement, reporting and verification (MRV) systems for REDD+. *Carbon Balance Manag*. 2017;12:9. <https://doi.org/10.1186/s13021-017-0078-9>.
71. Mondo JM, Chuma GB, Muke MB, et al. Utilization of non-timber forest products as alternative sources of food and income in the highland regions of the Kahuzi-Biega National Park, eastern Democratic Republic of Congo. *Trees Forests People*. 2024. <https://doi.org/10.1016/j.tfp.2024.100547>.
72. Mudinga ME, Ngendakumana S, Ansoms A. Analyse critique du processus de cogestion du parc national de Kahuzi-Biega en République Démocratique du Congo. *La revue électronique en sciences de l'environnement* 17; 2013.
73. Murcia C. Edge effects in fragmented forests: implications for conservation. *Trends Ecol Evol*. 1995;10:58–62. [https://doi.org/10.1016/S0169-5347\(00\)88977-6](https://doi.org/10.1016/S0169-5347(00)88977-6).
74. Nackoney J, Molinario G, Potapov P, et al. Impacts of civil conflict on primary forest habitat in northern Democratic Republic of the Congo, 1990–2010. *Biol Conserv*. 2014;170:321–8. <https://doi.org/10.1016/j.biocon.2013.12.033>.
75. Oliveira PJC, Asner GP, Knapp DE, et al. Land-use allocation protects the Peruvian Amazon. *Science*. 2007;317:1233–6. <https://doi.org/10.1126/science.1146324>.
76. Panta M, Kim K, Joshi C. Temporal mapping of deforestation and forest degradation in Nepal: applications to forest conservation. *For Ecol Manag*. 2009;256:1587–95. <https://doi.org/10.1016/j.foreco.2008.07.023>.
77. Pir Bavaghar M. Deforestation modelling using logistic regression and GIS. *J For Sci*. 2015;61:193–9. <https://doi.org/10.1722/1/78/2014-JFS>.
78. Plumptre AJ, Behangana M, Davenport T, et al. Albertine Rift Biodiversity, WCS. 2003.
79. Plumptre AJ, Nixon S, Kujirakwinja DK, et al. Catastrophic decline of world's largest primate: 80% loss of Grauer's gorilla (*Gorilla beringei graueri*) population justifies critically endangered status. *PLoS ONE*. 2016;11:e0162697. <https://doi.org/10.1371/journal.pone.0162697>.
80. Potapov P, Hansen MC, Laestadius L, et al. The last frontiers of wilderness: tracking loss of intact forest landscapes from 2000 to 2013. 2017. *Sci Adv*. <https://doi.org/10.1126/sciadv.1600821>.
81. Potapov PV, Turubanova SA, Hansen MC, et al. Quantifying forest cover loss in Democratic Republic of the Congo, 2000–2010, with Landsat ETM+ data. *Remote Sens Environ*. 2012;122:106–16. <https://doi.org/10.1016/j.rse.2011.08.027>.
82. Prevedello JA, Vieira MV. Does the type of matrix matter? A quantitative review of the evidence. *Biodivers Conserv*. 2010;19:1205–23. <https://doi.org/10.1007/s10531-009-9750-z>.
83. Qin Y, Xiao X, Wigner J-P, et al. Carbon loss from forest degradation exceeds that from deforestation in the Brazilian Amazon Author list. *Nat Clim Change*. 2022;36:405–9.
84. Riitters K, Wickham J, Oneill R, et al. Global-scale patterns of forest fragmentation. *Conserv Ecol*. 2000;4:33.
85. Riitters KH, Wickham JD, O'Neill RV, et al. Fragmentation of continental United States forests. *Ecosystems*. 2002;5:815–22. <https://doi.org/10.1007/s10021002-0209-2>.

86. Shafeian E, Fassnacht F, Latifi H. Using Landsat Time Series to detect forest degradation in semi-arid areas. 2023.
87. Shapiro A, Grantham HS, Aguilar-Amuchastegui N, et al. Forest condition in the Congo Basin for the assessment of ecosystem conservation status. 2020.
88. Shapiro AC, Aguilar-Amuchastegui N, Hostert P, Bastin JF. Using fragmentation to assess degradation of forest edges in Democratic Republic of Congo. *Carbon Balance Manag.* 2016. <https://doi.org/10.1186/s13021-016-0054-9>.
89. Shapiro AC, Bernhard KP, Zenobi S, et al. Proximate causes of forest degradation in the Democratic Republic of the Congo vary in space and time. *Front Conserv Sci.* 2021. <https://doi.org/10.3389/fcosc.2021.690562>.
90. Shapiro AC, Grantham HS, Aguilar-Amuchastegui N, et al. Forest condition in the Congo Basin for the assessment of ecosystem conservation status. *Ecol Indic.* 2021. <https://doi.org/10.1016/j.ecolind.2020.107268>.
91. Slagter B, Reiche J, Marcos D, et al. Monitoring direct drivers of small-scale tropical forest disturbance in near real-time with Sentinel-1 and -2 data. *Remote Sens Environ.* 2023;295:113655. <https://doi.org/10.1016/j.rse.2023.113655>.
92. Souza C Jr, Tenneson K, Digler J, et al. Forest degradation and deforestation. In: Cardille JA, et al., editors. *Cloud-based remote sensing with google earth engine*. Berlin: Springer; 2024.
93. Spira C, Kirkby A, Kujirakwinja D, Plumtre AJ. The socio-economics of artisanal mining and bushmeat hunting around protected areas: Kahuzi-Biega National Park and Itombwe Nature Reserve, eastern Democratic Republic of Congo. *Oryx.* 2019;53:136–44. <https://doi.org/10.1017/S003060531600171X>.
94. Spira C, Mitamba G, Kirkby A, et al. Inventaire de la biodiversité dans le Parc National de Kahuzi-Biega, République Démocratique du Congo. 2018.
95. Taiyun Wei M, Taiyun Wei cre A, Simko aut V, et al. Package "corrplot": Visualization of a Correlation Matrix. 2022.
96. Tchatchou B, Sonwa DJ, Tiani AM. Deforestation and forest degradation in the Congo Basin State of knowledge, current causes and perspectives. 2015.
97. Thies C, Rosoman G, Cotter J, Frigne J. Les paysages de forêts intactes Pourquoi il est essentiel de préserver ces forêts de toute exploitation industrielle. Amsterdam. 2011.
98. Trani MK, Giles RH. An analysis of deforestation: metrics used to describe pattern change. *For Ecol Manag.* 1999;114:459–70.
99. Turner MG, Gardner RH. Landscape metrics. In: *Landscape ecology in theory and practice*. New York: Springer; 2015. p. 97–142.
100. Turubanova S, Potapov PV, Tyukavina A, Hansen MC. Ongoing primary forest loss in Brazil, Democratic Republic of the Congo, and Indonesia. *Environ Res Lett.* 2018;13:074028. <https://doi.org/10.1088/1748-9326/aacd1c>.
101. Tyukavina A, Hansen MC, Potapov P, et al. Congo basin forest loss dominated by increasing smallholder clearing. *Sci Adv.* 2018. <https://doi.org/10.1126/sciadv.aat2993>.
102. IUCN. Guidelines for using A global standard for the identification of Key Biodiversity Areas: version 1.2. IUCN, International Union for Conservation of Nature. 2022.
103. IUCN. Rapport de la mission conjointe de suivi réactif Centre du patrimoine mondial/IUCN au Parc National de Kahuzi-Biega. 2017.
104. UNEP. Africa Mountains Atlas. Nairobi. 2014.
105. UNESCO. Convention concernant la protection du patrimoine mondial, culturel et naturel. Paris. 1972.
106. Useni Sikuzani Y, Mpanda Mukenza M, Khoji Muteya H, et al. Vegetation fires in the Lubumbashi charcoal production basin (The Democratic Republic of the Congo): drivers, extent and spatiotemporal dynamics. *Land.* 2023;12(12):2171. <https://doi.org/10.3390/land12122171>.
107. Vancutsem C, Achard F, Pekel J-F, et al. Long-term (1990–2019) monitoring of forest cover changes in the humid tropics. *Sci Adv.* 2021. <https://doi.org/10.1126/sciadv.abe1603>.
108. Venter O, Sanderson EW, Magrath A, et al. Sixteen years of change in the global terrestrial human footprint and implications for biodiversity conservation. *Nat Commun.* 2016. <https://doi.org/10.1038/ncomms12558>.
109. Welsink A-J, Dupuis C, Cue La Rosa L, et al. Monitoring fine-scale natural and logging-related tropical forest degradation using Sentinel-1. *Remote Sens Environ.* 2025;328:114878. <https://doi.org/10.1016/j.rse.2025.114878>.
110. Wickham H. *ggplot2: Elegant graphics for data analysis*. Cham: Springer; 2016.
111. Wilkinson L, Friendly M. The history of the cluster heat map. *Am Stat.* 2009;63:179–84. <https://doi.org/10.1198/tas.2009.0033>.
112. WWF-PARAP. Le réseau des aires protégées de la République démocratique du Congo. 2021. <https://www.wwf.de/fileadmin/fm-wwf/Publikationen-PDF/Afrika/WWF-Parap-Poster-French.pdf>. Accessed 6 Dec 2023.
113. Yuh YG, N'Goran KP, Kross A, et al. Monitoring forest cover and land use change in the Congo Basin under IPCC climate change scenarios. *PLoS ONE.* 2024. <https://doi.org/10.1371/journal.pone.0311816>.
114. Zhao C, Pan Y, Zhu X, et al. Monitoring of deforestation events in the tropics using multidimensional features of Sentinel 1 radar data. *Front Forests Glob Change.* 2023. <https://doi.org/10.3389/ffgc.2023.1257806>.
115. Zhou L, Dang X, Sun Q, Wang S. Multi-scenario simulation of urban land change in Shanghai by random forest and CA-Markov model. *Sustain Cities Soc.* 2020. <https://doi.org/10.1016/j.scs.2020.102045>.
116. Zhuravleva I, Turubanova S, Potapov P, et al. Satellite-based primary forest degradation assessment in the Democratic Republic of the Congo, 2000–2010. *Environ Res Lett.* 2013;8:024034. <https://doi.org/10.1088/1748-9326/8/2/024034>.

## Publisher's Note

Springer Nature remains neutral with regard to jurisdictional claims in published maps and institutional affiliations.